Automated Design of Aerogravity-Assist Trajectories

Eugene P. Bonfiglio* and James M. Longuski[†]
Purdue University, West Lafayette, Indiana 47907-1282
and
Nguyen X. Vinh[‡]
University of Michigan, Ann Arbor, Michigan 48109-2140

Aerogravity assist enhances the technique of gravity assist through the use of a lifting vehicle that flies through the atmosphere of the swingby planet. An algorithm is developed that automatically searches for such trajectories to destination planets including Pluto, Neptune, Saturn, Mars, and Venus. Trajectories for lift-to-drag (L/D) ratios ranging from 1 to 10 are calculated using Venus and Mars as aerogravity-assist flyby bodies. Current waverider technology promises to deliver L/D ratios as high as 7. Trajectories to Pluto with times of flight near 8 years and launch C_3 (excess velocity squared) under 56 km²/s² are presented for L/D ratios of 7. This techniques significantly reduces launch energy and the time of flight for many missions, enabling greater access to solar system bodies.

Nomenclature

C_D = coefficient of drag
C_{D_0} = zero-lift drag coefficient
C_L = coefficient of lift
C_3 = hyperbolic excess velocity squared, km²/s²
D = drag, N
E = lift-to-drag ratio
g = varying acceleration due to gravity, m/s²
K = correction factor for drag equation
L = lift, N
m = vehicle mass, kg
r = radius from center of planet to spacecraft, km
S = lifting body reference area, m²
u = dimensionless speed variable, ratio of speed squared over local circular orbit speed squared
V = velocity, km/s
V_∞ = hyperbolic excess velocity, km/s
γ = flight-path angle (positive upward from the local horizontal), deg
η = dimensionless glide-altitude parameter
θ = aerodynamic turn angle, deg
μ = gravitational parameter (constant for a given planet), km³/s²
ρ = atmospheric density, kg/m³
ϕ = total turn angle, deg

Subscripts

$-$ = incoming state
$+$ = outgoing state

Introduction

THE concept of aerogravity assist (AGA) was being considered nearly 20 years ago at the Jet Propulsion Laboratory (JPL) as a method of augmenting gravity assist[1] (see Fig. 1). A lifting body flies through the atmosphere of a planet with the lift vector oriented toward the center of the planet. This negative lift allows

the spacecraft to remain at a desired constant altitude, hence turning the V_∞ vector more than the gravity assist alone. Even though the drag reduces the spacecraft's velocity, the vehicle can still achieve a net gain in ΔV because the V_∞ turning associated with an AGA is far greater than the turning obtained in a pure gravity assist. With AGA, we anticipate trajectories to Pluto with times of flight as low as 5–7 years and Solar Probe missions with final orbit periods of 0.7 year (Ref. 2).

Drag losses can be alleviated by a high-lift-to-drag vehicle such as the waverider, first introduced by Nonweiler in 1959.[3] This class of vehicles is theorized to have very high L/D ratios at hypersonic speeds. Current tests and measurements put the L/D ratio at about 5–7 (Ref. 4). An assessment of heating for a blunt leading edge on the waverider is presented by Lewis and McRonald.[5]

Present literature does not account precisely for drag effects in AGA trajectories. Bender,[6] McRonald and Randolph,[2] and Randolph and McRonald[7] present trajectory possibilities, but do not calculate drag losses, and provide only a few specific launch dates. Sims[8] does a thorough trajectory search for AGA possibilities where he assumes an infinite L/D ratio and later provides analytic approximations of drag effects. In this paper, we develop an algorithm for trajectory analysis that quickly and accurately models the drag loss effects of an AGA. The AGA algorithm opens the door for trajectory design studies of combinations of AGA planets.

Analytic Theory for Aerogravity Assist

We develop the theory for AGA maneuvers, starting from the basic two-dimensional equations of motion for a nonthrusting, lifting body in the atmosphere[9]:

$$\dot{r} = V \sin \gamma \qquad (1)$$

$$\dot{\theta} = (V \cos \gamma)/r \qquad (2)$$

$$\dot{V} = -(D/m) - g \sin \gamma \qquad (3)$$

$$V\dot{\gamma} = L/m - g \cos \gamma + (V^2/r) \cos \gamma \qquad (4)$$

where the equations for drag and lift are

$$D = \tfrac{1}{2}\rho S V^2 C_D, \qquad L = \tfrac{1}{2}\rho S V^2 C_L \qquad (5)$$

The general equation for the drag polar takes the form

$$C_D = C_{D_0} + K |C_L|^n \qquad (6)$$

Traditionally a parabolic drag polar is used ($n = 2$), although the best model available in the literature uses $n = 1.75$ for a waverider.[4] Because n may vary for different lifting bodies, we derive the exact
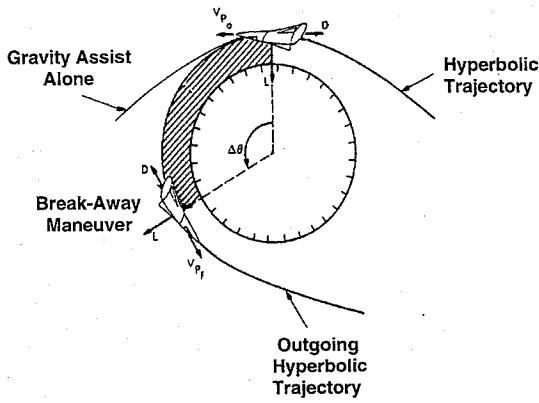
Fig. 1 Aerogravity assist (adapted from Ref. 1).

AGA equations of motion for the general drag polar [Eq. (6)], as well as the parabolic case. For convenience, we introduce E as the lift-to-drag ratio. Using the lift and drag equations, we write

$$E = L/D = C_L/C_D = C_L/\left(C_{D_0} + K|C_L|^n\right) \qquad (7)$$

To calculate the maximum lift-to-drag ratio E^*, we set

$$\frac{dE}{dC_L} = \frac{\left(C_{D_0} + KC_L^n\right) - C_L\left(nKC_L^{n-1}\right)}{\left(C_{D_0} + KC_L^n\right)^2} = 0 \qquad (8)$$

which yields

$$C_L = C_L^* = \sqrt[n]{\frac{C_{D_0}}{(n-1)K}}, \qquad E^* = \frac{\sqrt[n]{(n-1)^{n-1}}}{n\sqrt[n]{KC_{D_0}^{n-1}}} \qquad (9)$$

We note that C_L^* does not represent a maximum value of C_L but rather the value of C_L at maximum E, that is, E^*. Setting $\dot{\gamma} = \gamma = 0$ in Eq. (4), we deduce the condition for constant altitude:

$$L = \tfrac{1}{2}\rho S V^2 C_L = mg - mV^2/r \qquad (10)$$

At this point, it is convenient to use the following dimensionless parameter and variable:

$$\eta = (\rho S r/2m)\sqrt[n]{C_{D_0}/[(n-1)K]} = (\rho S r/2m)C_L^*$$

$$u = rV^2/\mu = V^2/(gr) \qquad (11)$$

where η is a parameter specifying the glide altitude and u is the new speed variable. Using the definitions for η and u, and rearranging Eq. (10), we obtain the equilibrium condition for glide at constant altitude:

$$\eta\left(C_L/C_L^*\right) = (1-u)/u \qquad (12)$$

We note that $u = 2$ gives $V = \sqrt{(2\mu/r)}$, the escape velocity with respect to the AGA body. Because the spacecraft orbit is always hyperbolic with respect to the planet during an AGA (and η and C_L^* are greater than 0), it is clear from Eq. (12) that $C_L < 0$ during the entire maneuver. The maximum flythrough height h_{max} during the AGA maneuver can easily be found by setting $C_L = -C_{L max}$ in Eq. (12). We also note that Eq. (12) is independent of the drag equation and is completely general. Recalling that $\gamma = 0$ during the maneuver, Eqs. (2) and (3) become

$$\frac{d\theta}{dt} = \frac{V}{r}, \qquad \frac{dV}{dt} = \frac{-\rho S V^2 C_D}{2m} \qquad (13)$$

Combining these equations gives

$$\frac{dV}{d\theta} = \frac{-\rho S r V^2 C_D}{2mV} \qquad (14)$$

Taking the first derivative of V^2 with respect to θ, we get

$$\frac{d(V^2)}{d\theta} = 2V\left(\frac{dV}{d\theta}\right) = \frac{-\rho S r V^2 C_D}{m} \qquad (15)$$

Recalling the definition of u, we see that

$$\frac{du}{d\theta} = \left(\frac{r}{\mu}\right)\frac{d(V^2)}{d\theta} = \frac{-\rho S V^2 C_D}{mg} \qquad (16)$$

Substituting Eqs. (11) and (12) into Eq. (16) and simplifying yields

$$d\theta = \frac{-\tfrac{1}{2}(C_L/C_D)\,du}{1-u} \qquad (17)$$

Integrating this equation requires knowledge of C_L/C_D as a function of u. Using the general drag polar,

$$C_D = C_{D_0} + K|C_L|^n = C_{D_0}\left(1 + K|C_L|^n/C_{D_0}\right) \qquad (18)$$

and rearranging Eq. (9) gives

$$\left(C_L^*\right)^n = C_{D_0}/[(n-1)K] \qquad (19)$$

Dividing C_L by Eq. (18) and simplifying, we write C_L/C_D as

$$C_L/C_D = nE^*\left(C_L/C_L^*\right)(n-1)^{-1}\left[1 + |C_L/C_L^*|^n/(n-1)\right]^{-1} \qquad (20)$$

Finally, we use Eq. (12) to determine the C_L/C_D dependence on u:

$$C_L/C_L^* = (1-u)/(\eta u) \Rightarrow |C_L/C_L^*| = (u-1)/(\eta u) \qquad (21)$$

and, therefore,

$$\frac{C_L}{C_D} = \frac{nE^*(n-1)^{-1}(1-u)(\eta u)^{-1}}{1 + [(u-1)/(\eta u)]^n/(n-1)} \qquad (22)$$

Substituting Eq. (22) into Eq. (17) gives the following differential:

$$d\theta = -\tfrac{1}{2}E^* n\eta^{n-1}u^{n-1}[(n-1)\eta^n u^n + (u-1)^n]^{-1}\,du \qquad (23)$$

Equation (23) is the exact differential equation for the turn angle associated with the aerodynamic portion of an AGA maneuver. Hereafter, we refer to θ as the aerodynamic turn angle and to the solution to Eq. (23) as the general solution. Although Eq. (23) is general, it cannot be integrated explicitly for arbitrary values of n and, therefore, is impractical in developing a computationally fast algorithm. However, if we assume a value of $n = 2$, that is, the parabolic drag polar, then Eq. (23) becomes

$$\int_0^\theta d\theta = \int_{u_1}^{u_2} -E^* \eta u[(1+\eta^2)u^2 - 2u + 1]^{-1}\,du \qquad (24)$$

which can be integrated to provide

$$\theta = E^*\eta[2(1+\eta^2)]^{-1}\ell_n\left[\frac{(1+\eta^2)u_1^2 - 2u_1 + 1}{(1+\eta^2)u_2^2 - 2u_2 + 1}\right]$$

$$+ E^*[(1+\eta^2)]^{-1}\left\{\tan^{-1}\left[\frac{(1+\eta^2)u_1 - 1}{\eta}\right]\right.$$

$$\left. - \tan^{-1}\left[\frac{(1+\eta^2)u_2 - 1}{\eta}\right]\right\} \qquad (25)$$

Equation (25) can be simplified further using the trigonometric identity for $\tan(\alpha - \beta)$, to yield

$$\theta = E^*\eta[2(1+\eta^2)]^{-1}\ell_n\left[\frac{(1+\eta^2)u_1^2 - 2u_1 + 1}{(1+\eta^2)u_2^2 - 2u_2 + 1}\right]$$

$$+ E^*(1+\eta^2)^{-1}\tan^{-1}\left[\frac{\eta(u_1 - u_2)}{(1+\eta^2)u_1 u_2 - (u_1 + u_2) + 1}\right] \qquad (26)$$

Equation (26) is the exact solution for the aerodynamic turn angle of an AGA where the lifting body has a parabolic drag polar. We will refer to Eq. (26) as the parabolic solution.

Realistically, in hypersonic flight,[10] the exponent n takes on the value $n = \frac{3}{2}$. In this case, Eq. (23) becomes

$$d\theta = -ku^{\frac{1}{2}}\left[au^{\frac{3}{2}} + (u-1)^{\frac{3}{2}}\right]^{-1} du \qquad (27)$$

where

$$k = \frac{3}{4}E^*\eta^{\frac{1}{2}}, \qquad a = \frac{1}{2}\eta^{\frac{3}{2}} \qquad (28)$$

We rewrite Eq. (27) to get

$$d\theta = -ku\left[au^2 + (u-1)\sqrt{u(u-1)}\right]^{-1} du \qquad (29)$$

Using the change of variable

$$u = -x^2/(2x+1) \qquad (30)$$

in Eq. (27) results in the following dependence of θ on x:

$$d\theta = -2kx^3(x+1)\left((2x+1)^3\left\{\frac{ax^4}{(2x+1)^2}\right.\right.$$
$$\left.\left. - \left[\frac{(x+1)^2}{2x+1}\right]\sqrt{\frac{x^2(x+1)^2}{(2x+1)^2}}\right\}\right)^{-1} dx \qquad (31)$$

During supercircular motion, the lift must be negative requiring u to be greater than unity. When $1 < u < \infty$, we get $x < 0$, $(x+1) > 0$, and $(2x+1) < 0$. Using this knowledge, we can simplify Eq. (31) to obtain

$$d\theta = -2kx^2(x+1)[(2x+1)\{(1-a)x^3 + 3x^2 + 3x + 1\}]^{-1} dx \qquad (32)$$

On integrating,

$$\theta = 2k[I(x_2) - I(x_1)] \qquad (33)$$

We begin integrating Eq. (32) by breaking the fraction up into the following sum:

$$\frac{1}{(1+a)(2x+1)} + \left(\frac{ax^2 - x - 1}{1+a}\right)[(1-a)x^3 + 3x^2 + 3x + 1] \qquad (34)$$

Next we note that

$$x = 1/\left(a^{\frac{1}{3}} - 1\right) \qquad (35)$$

is a real root of

$$(1-a)x^3 + 3x^2 + 3x + 1 = 0 \qquad (36)$$

Defining ϵ as

$$\epsilon = a^{\frac{1}{3}} \qquad (37)$$

allows the fraction

$$\frac{ax^2 - x - 1}{(1-a)x^3 + 3x^2 + 3x + 1} \qquad (38)$$

to be rewritten as

$$(\epsilon^3 x^2 - x - 1)/\{[x + 1/(1-\epsilon)][(1-\epsilon^3)x^2$$
$$+ (1-\epsilon)(2+\epsilon)x + (1-\epsilon)]\} \qquad (39)$$

which can be decomposed to provide

$$A/[x + 1/(1-\epsilon)] + (Bx + C)/[(1-\epsilon^3)x^2$$
$$+ (1-\epsilon)(2+\epsilon)x + (1-\epsilon)] \qquad (40)$$

where

$$A = \frac{1 - \epsilon + \epsilon^2}{3\epsilon(1-\epsilon)} \qquad (41)$$

$$B = \frac{(\epsilon^2 - 1)(2\epsilon^2 + 1)}{3\epsilon} \qquad (42)$$

$$C = \frac{-(1-\epsilon)(1+\epsilon)^2}{3\epsilon} \qquad (43)$$

Using Eqs. (34) and (40), we can break Eq. (32) into three separate fractions, integrate and obtain

$$I(x) = I_1(x) + I_2(x) + I_3(x) \qquad (44)$$

where

$$I_1(x) = \{1/[2(1+a)]\}\,\ell_n(2x+1) \qquad (45)$$

$$I_2(x) = \frac{1 - \epsilon + \epsilon^2}{3\epsilon(1-\epsilon)(1+\epsilon^3)}\,\ell_n\left(x + \frac{1}{1-\epsilon}\right) \qquad (46)$$

$$I_3 = \frac{-(1+\epsilon)(2\epsilon^2+1)}{6\epsilon(1+\epsilon+\epsilon^2)(1+\epsilon^3)}\,\ell_n[(1-\epsilon^3)x^2 + (1-\epsilon)(2+\epsilon)x$$
$$+ (1-\epsilon)] - \left[\frac{1+\epsilon}{\sqrt{3}\epsilon(1+\epsilon+\epsilon^2)(1+\epsilon^3)}\right]$$
$$\times \tan^{-1}\left[\frac{2(1+\epsilon+\epsilon^2)x + (2+\epsilon)}{\sqrt{3}\epsilon}\right] \qquad (47)$$

Computationally, the parabolic and hypersonic solutions have the disadvantage of not explicitly providing the outgoing velocity when the incoming velocity and aerodynamic turn angle are known. To obtain such an equation, we need to start over from Eq. (17).

If we assume the L/D ratio remains close to the maximum value during the entire trajectory,[7] then we can set $C_L/C_D = -E^*$ in Eq. (17) and integrate to obtain

$$\theta = -\frac{1}{2}E^*\,\ell_n[(u_2 - 1)/(u_1 - 1)] \qquad (48)$$

Defining $u_\infty = V_\infty^2/(\mu/r)$ and noticing that $u = 2 + u_\infty$, we can solve Eq. (48) for the exit condition u_∞^+ as a function of the incoming condition u_∞^-,

$$u_\infty^+ = \left(u_\infty^- + 1\right)e^{-2\theta/E^*} - 1 \qquad (49)$$

A similar form is given by Lewis and McRonald,[5] although they do not use dimensionless variables, as follows:

$$V_\infty^{+^2} = \exp(-2\theta/E^*)V_\infty^{-^2} + \{[\exp(-2\theta/E^*) - 1](\mu/r)\} \qquad (50)$$

Equation (49), or equivalently Eq. (50), is only an approximate solution for constant L/D glide. However, this approximate solution provides an accurate estimate of the exit condition.

Numerical comparisons of the general solution [Eq. (23)] with $n = 1.75$ (Ref. 4), the parabolic solution [Eq. (26)], and the constant L/D solution [Eq. (48)] are performed by Bonfiglio.[11] Compared to the general solution for a typical AGA at Venus, the difference in V^+ (with respect to Venus) is only 0.06 km/s for the parabolic solution (where $n = 2$) and 0.05 km/s for the constant L/D solution. These discrepancies are very small, which means that we can use either closed-form solution for the basis of our AGA algorithm. We choose the latter, Eq. (49) [or Eq. (50)], because of its simplicity. Any error produced by this model can be removed by a relatively simple guidance law during the atmospheric flythrough.[11]

Automated AGA Search Method

Using the constant L/D solution, we develop an algorithm suitable for installation into the Satellite Tour Design Program[12] (STOUR). STOUR was originally developed at JPL where it was used interactively to design the Galileo Orbiter Tour. The program was upgraded at Purdue University to perform automated design for a variety of gravity-assist missions.
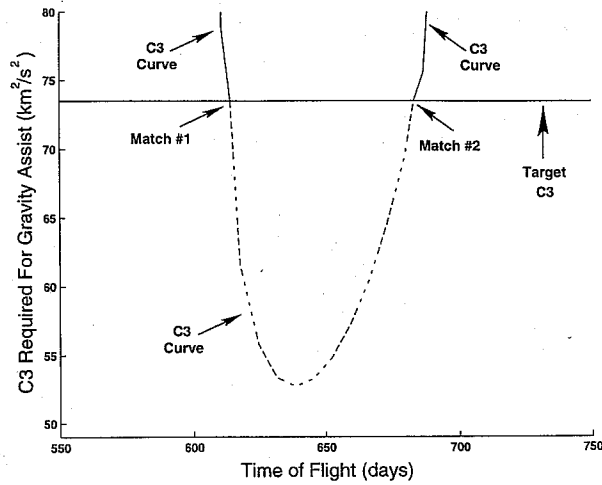
Fig. 2 C_3 curve for a Venus-to-Earth C_3 matching problem.

Fig. 3 L/D curve for a Venus-to-Earth L/D matching problem.

C_3 Matching

STOUR patches gravity-assist trajectories together by the method[13,14] of C_3 matching, where C_3 is the hyperbolic excess velocity squared (V_∞^2). The C_3 matching problem involves matching the magnitude of the incoming V_∞ (with respect to the particular satellite or planet in question) with the magnitude of an outgoing V_∞, to effect encounter with the next satellite (or planet) in the trajectory path. STOUR accomplishes this by first determining the range of time of flight from the current gravity-assist body to the target body. For example, suppose the time of flight range is 0–225 days. This time range is broken up into 20 intervals to the target body. STOUR then solves the Lambert problem from the current flyby body to the target body for each time of flight interval. (In the case of a heliocentric trajectory, a conic solution is found with the sun as the attracting center.) Each solution to the Lambert problem supplies a particular outgoing V_∞. When the magnitude of one of the outgoing V_∞ vectors is relatively close to the magnitude of the incoming V_∞ vector, a C_3 match is found using a root solver.

Figure 2 presents a C_3 curve for trajectories from Venus to Earth. The horizontal line represents the magnitude of the incoming C_3 at Venus (target C_3). Because the horizontal line intersects the C_3 curve twice, we know that there are two matches for trajectories to Earth.

L/D Matching

In developing the new version of STOUR, our goal was to install an AGA algorithm requiring the fewest modifications to STOUR. In this way, we minimize new programming and reduce chances of introducing errors into the code. This problem is solved by implementing a routine we refer to as L/D matching. This routine is based on the following equation[4]:

$$\theta = \phi - \sin^{-1}\left[1/\left(1 + u_\infty^-\right)\right] - \sin^{-1}\left[1/\left(1 + u_\infty^+\right)\right] \quad (51)$$

where θ is the aerodynamic turn angle and ϕ is the total turn angle of the V_∞ vector. This equation can be combined with Eq. (50) to solve for E^* to yield

$$E^* = 2\left\{\ell_*\left[\left(1 + u_\infty^-\right)/\left(1 + u_\infty^+\right)\right]\right\}^{-1}\left\{\phi - \sin^{-1}\left[1/\left(1 + u_\infty^-\right)\right]\right.$$

$$\left. - \sin^{-1}\left[1/\left(1 + u_\infty^+\right)\right]\right\} \quad (52)$$

The most convenient advantage of the L/D matching algorithm is its reliance on the C_3 matching algorithm. In Fig. 2, the dotted portion of the C_3 curve represents the C_3 values below the target C_3 line. Each of the outgoing V_∞ (on the dotted line) has a lower magnitude with respect to the incoming V_∞ (this difference can be considered a result of drag). Therefore, any point on the C_3 curve below the incoming C_3 line has an L/D value associated with it according to Eq. (52). Performing this calculation on all of the points below the C_3 line in Fig. 2, and plotting the L/D values, we obtain Fig. 3. Note
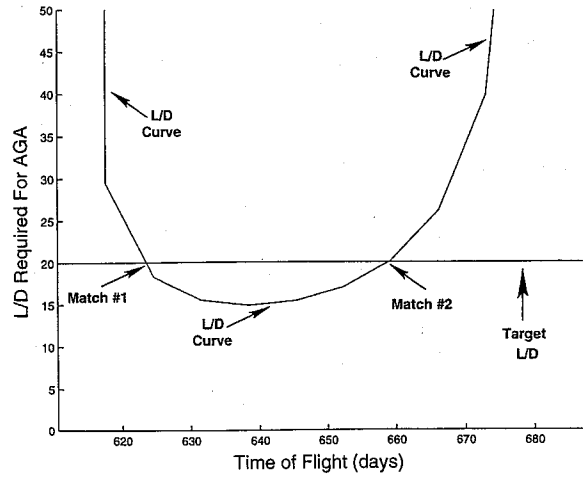
that, because the C_3 curve will tend to have very few points below the incoming C_3 line, the L/D curve is more segmented, that is, less smooth. The L/D plot includes a horizontal target line that represents the L/D capability of the waverider. Thus, if our waverider has an L/D of 20, then the horizontal line represented by that value gives, by its intersection with the L/D curve, the conic trajectory to the target planet. In Fig. 3, for example, we have two intersections (match 1 and match 2) corresponding to two conic trajectories with times of flight of 625 and 660 days, respectively. On the other hand, if the L/D capability was less than 10, Fig. 3 shows that there would be no trajectories because the value of 10 falls entirely below the L/D curve. This algorithm is verified through numerical methods.[11]

AGA Missions

Next, we perform trajectory design studies of the AGA planets and of L/D ratios for various missions. Our goal is to determine the savings AGA maneuvers can provide in terms of time of flight and propellant.

One mission of great interest for the past few decades is a Pluto flyby. A Neptune orbiter might also be very interesting, especially if AGA is able to reduce the total ΔV and time of flight required. Currently, a number of missions are being planned to Mars. Cheaper free-return trajectories that can obtain atmospheric samples would provide valuable science. In a similar manner, Venus free-return trajectories would be scientifically interesting. AGA sample-return missions from the gas giants (such as Saturn) could determine the age of these distant planets.
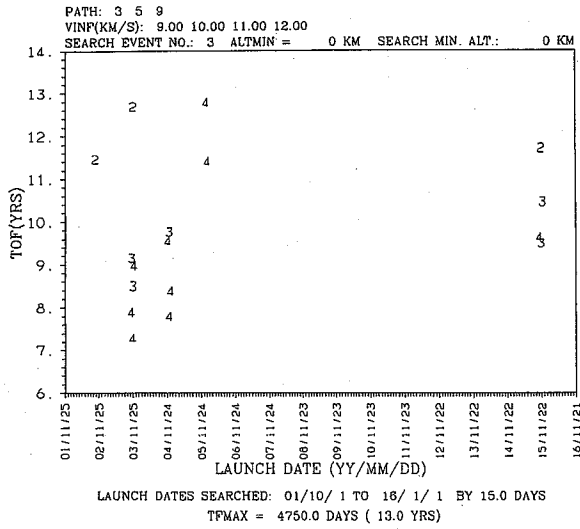
Here we investigate missions using Venus and Mars for aerogravity assists. Randolph and McRonald[7] found the combination of Venus and Mars for AGA to be extremely beneficial. Table 1 lists the missions we analyze as well as the paths, and the L/D ratios allowed for each path. (When multiple AGA bodies are used, the L/D ratio is the same at all of the bodies.) Note that in both the Pluto and Neptune case, we also use paths of just Mars and just Venus to determine the necessity of an AGA at both Venus and Mars. One of our main objectives is to determine the L/D ratios required for AGA missions to become attractive. To estimate this value, we use a wide range of L/D ratios including very low L/D ratios. For the Mars and Venus trajectories, the L/D ratio of 1 may be achievable with off-the-shelf technology. At the other end of the scale, waveriders represent cutting-edge technology currently at $L/D = 5$, with promise for $L/D = 7$ in the near future.

Pluto Missions

Pluto is the only planet that has not been visited by spacecraft. For this reason, a mission to Pluto is very exciting and very much in demand by scientists. The original baseline trajectory for the Pluto Express[8,15] had a time of flight of 12.0 years and a total $\Delta V = 6.18$ km/s (an equivalent launch V_∞ of 8.6 km/s), where the ΔV is that of injection from circular orbit plus deep space ΔV. The

Table 1 Search paths and L/D ratios for AGA missions

Mission	L/D ratios	Paths searched
Neptune	5, 7, 10	M, V, VM, VMVJ, VMS VMU, VMJS, VVM
Pluto	5, 7, 10	M, V, VM, VMJ VMS, VMU, VMJS
Mars free return	1, 3, 5, 7	M, MV, VM
Venus free return	1, 3, 5, 7	M, MV, VM
Saturn free return	5, 7, 10	VMS

PATH: 3 5 9
VINF(KM/S): 9.00 10.00 11.00 12.00
SEARCH EVENT NO.: 3 ALTMIN =   0 KM   SEARCH MIN. ALT.:   0 KM

LAUNCH DATES SEARCHED: 01/10/ 1 TO 16/ 1/ 1 BY 15.0 DAYS
TFMAX = 4750.0 DAYS (13.0 YRS)

Fig. 4 Pure gravity-assist trajectories to Pluto comparable to the 2004 baseline mission.

current mission to Pluto (now termed Pluto–Kuiper) uses a gravity assist from Jupiter to achieve a time of flight of 8 years.

Figure 4 gives results of an STOUR search for pure gravity-assist trajectories to Pluto that are comparable to the current baseline mission. The legend for launch-date plots is as follows. PATH indicates the planets encountered, including launch and destination bodies, for example, PATH: 3 5 9 uses a Jupiter gravity assist from Earth to Pluto. VINF is the launch V_∞. The numerals 1, 2, 3, 4, etc., on the plot represent the first, second, third, fourth, etc., V_∞ in the list. If an AGA maneuver is used during the trajectory, then A, B, C, D, etc., is used instead of 1, 2, 3, 4, etc. For example, in Fig. 5 the D denotes a V_∞ of 12 km/s. For an STOUR–AGA plot, it is possible to have both AGA and pure gravity-assist points on each plot. LIFT/DRAG is the lift/drag ratio used at each AGA planet. If LIFT/DRAG = 0, then there was no AGA performed at that planet. For example, in Fig. 5, the PATH = 3 2 4 9 and the LIFT/DRAG = 0.0 7.0 7.0 0.0 means there is no AGA maneuver at the first and last planet in the path, but AGAs with LIFT/DRAG = 7 are possible at the second and third planets in the path. SEARCH EVENT NO. is the event in PATH for which data are plotted. For example, in Fig. 5, time of flight (TOF) to Pluto is plotted because encounter with Pluto is the fourth event in the PATH. ALTMIN is the minimum flyby altitude permitted in the STOUR run. SEARCH MIN. ALT. is minimum altitude. Trajectories with flyby altitudes below this value are not included in the plot. LAUNCH DATES SEARCHED provides the launch-date range used in the STOUR run. For example, 01/10/1 in the plot means 1 October 2001. The launch-date increment is also given, for example, by 15 days. TFMAX is the maximum allowable TOF in the STOUR run. We can clearly see from Fig. 4 that exactly 17 trajectories exist for the 15-year launch range searched (for launch V_∞ of 9–12 km/s). Figure 5 shows AGA results for the same range with AGAs at Venus and Mars and $L/D = 7$. The number of trajectories to Pluto for the AGA case is an order of magnitude larger than that of the pure gravity-assist case. This is an excellent example of how AGA not only decreases TOF and launch energy, but increases the number of launch oppor-

Table 2 Pluto trajectories

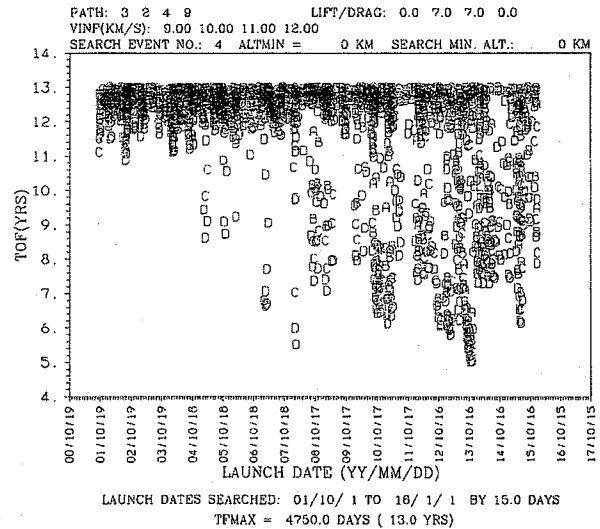| Parameter	Baseline mission[a]	Comparable AGA trajectories[b]
TOF, yr	8.0	5.0, 8.0
Launch V_∞, km/s	12.0	12.0, 7.45
L/D	——	7

[a]Jupiter gravity assist. [b]VM AGA.

Table 3 Trajectories to Pluto using AGA at Venus and Mars[a]

Path	Launch date	TOF, yr	Launch V_∞, km/s	Arrival V_∞, km/s	L/D
Low launch V_∞ and short TOF[b]					
VM	31 Oct. 2013	5.2	9.0	30.5	10
VM	16 Oct. 2013	7.2	7.0	21.0	10
VM	16 Oct. 2013	6.0	9.0	26.2	7
VM	13 Feb. 2014	9.2	7.0	19.9	7
VM	16 Oct. 2013	6.7	8.0	22.8	7
VM	16 Oct. 2013	7.2	9.0	21.1	5
VMS	9 June 2009	11.4	7.0	19.1	5
Low launch V_∞, short TOF, and low arrival V_∞[b]					
VM	16 Sept. 2013	8.6	7.0	17.2	10
VM	13 Feb. 2014	11.5	6.0	14.5	7
VM	17 Aug. 2013	9.6	8.0	15.1	7
VM	16 Oct. 2013	9.4	8.0	15.3	5
VMJS	20 Sept. 2015	12.9	6.0	13.6	5
Low launch V_∞ and low arrival V_∞[b]					
VM	1 Sept. 2013	10.8	7.0	12.9	10
VM	24 Feb. 2012	12.1	7.0	13.3	7
VM	31 Oct. 2013	12.8	8.0	10.3	5
VM	15 March 2014	12.0	7.0	13.5	5

[a]Jupiter and Saturn are used for gravity assist alone (i.e., not AGA).
[b]Measures of merit.

PATH: 3 2 4 9   LIFT/DRAG: 0.0 7.0 7.0 0.0
VINF(KM/S): 9.00 10.00 11.00 12.00
SEARCH EVENT NO.: 4 ALTMIN =   0 KM   SEARCH MIN. ALT.:   0 KM

LAUNCH DATES SEARCHED: 01/10/ 1 TO 16/ 1/ 1 BY 15.0 DAYS
TFMAX = 4750.0 DAYS (13.0 YRS)

Fig. 5 AGA trajectories to Pluto comparable to the 2004 baseline mission.

tunities. Table 2 gives two AGA trajectories (selected from Fig. 5) for comparison against the 2004 baseline mission. In the first example, if we use the same launch V_∞ for an AGA trajectory, then the TOF is reduced by 3 years (compared to the 8-year TOF of the baseline mission). Conversely, if we match the 8-year TOF with an AGA, we can reduce the required launch V_∞ by about 4.5 km/s. We conclude from these comparisons that aerogravity assist provides an advantageous tradeoff between TOF and total launch energy.

In mission design, the definition of "best" can sometimes be ambiguous. We use three sets of measures of merit when analyzing the STOUR–AGA data. The first is low launch V_∞ and short TOF, whereas the second seeks low values for TOF, launch V_∞, and arrival V_∞. The third measure of merit is low launch V_∞ and low arrival V_∞. Table 3 gives the best trajectories for each of the three sets of measures. Trajectories are listed for each of the L/D ratios

used in our search. Most of the trajectories listed in Table 4 use the Venus–Mars (VM) path. The Venus–Mars–Jupiter (VMJ) and Venus–Mars–Saturn (VMS) paths (with AGAs only at Venus and Mars) provide low launch V_∞, but the Jupiter and Saturn flybys increase the TOF. This increase in flight time indicates pure gravity assist at Jupiter or Saturn is no longer needed to get to Pluto because AGAs at Venus and Mars provide almost unlimited V_∞ turning. Table 3 shows a trajectory to Pluto with a TOF of only 7.2 years and a low launch V_∞ of 7 km/s for an L/D ratio of 10. This trajectory outperforms both of the earlier mentioned pure gravity-assist trajectories in flight time and total ΔV.
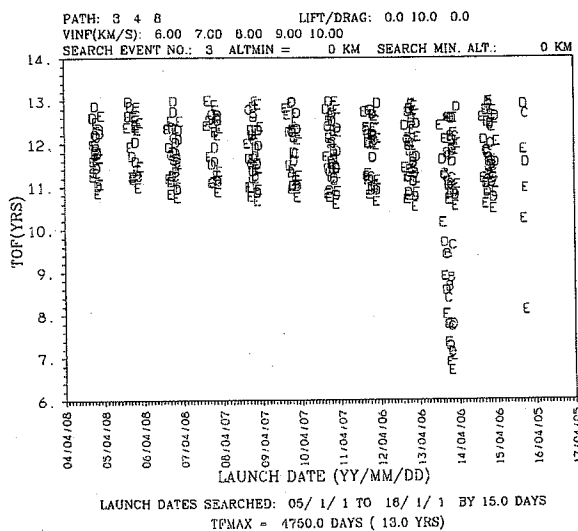
Neptune Missions

Neptune is a very interesting planet because it is the farthest gas giant from the sun. Our only contact with Neptune has been through Voyager II. Since then, the possibility of further exploration at Neptune has been discussed in the scientific community. For a Neptune orbiter, the arrival V_∞ for most viable trajectories is extremely high and costly because high arrival V_∞ translates into high orbit-insertion ΔV. One of the benefits of an AGA mission is that the lifting body used for the aerogravity assist can also be used for aerocapture at the destination planet.

Figure 6 presents STOUR–AGA results for a path to Neptune with AGAs at Venus and Mars. Trajectories are plotted as a function of arrival V_∞ (for launch V_∞ of 6 and 7 km/s). Plotting arrival V_∞ on the horizontal axis is useful for this analysis because it allows us to quickly find the best possible trajectory within the search parameters. (TOF vs launch date is not shown for the purposes of brevity.) Pluto trajectories are useful benchmarks for the Neptune analysis because these planets are at about the same distance from the sun for the dates searched. (We note, however, that Pluto is more difficult to reach because of its inclined orbit.) Again, Fig. 6 verifies that AGA provides many trajectories with low launch energies and short TOF. As might be expected, the shorter the TOF is, the higher the arrival V_∞, although this can also be a problem with pure gravity assist. As we show in the Mars free-return analysis, AGA can help reduce arrival V_∞.

Figure 7 plots trajectories to Neptune using aerogravity assist from Mars. Recall that a single AGA simplifies the waverider design process so that it is important to know what a single AGA can achieve. We see from Fig. 7 that it is possible to use only Mars, but
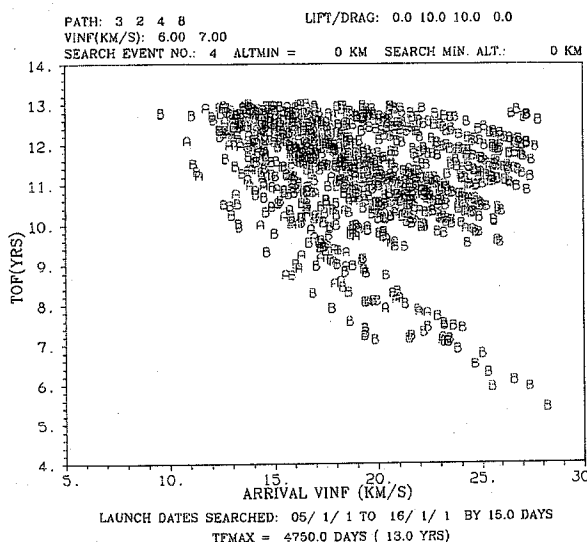
Fig. 6   Trajectories to Neptune via AGAs at both Venus and Mars.

Fig. 7   Trajectories to Neptune via AGA at Mars.

there are fewer opportunities. Using Venus in conjunction with Mars not only reduces launch energy and TOF, it increases the number of launch opportunities.

The best Neptune opportunities are listed in Table 4. It is apparent, that very short flight times are attainable even with L/D ratios of 5, provided a launch V_∞ of 7.0 km/s is used. Also very promising is that a spacecraft can reach Neptune with a low arrival V_∞ of nearly 9 km/s for $L/D = 5$. Trajectories with only a Mars AGA are also listed in Table 4. (These cannot be directly compared to the VM trajectories because an additional flyby, while reducing energy and TOF, increases the complexity of the waverider design.[5]) We note that, in Table 1, the VVM path was searched for Neptune missions. The second Venus flyby generally provides extra V_∞ turning during the trajectory, but this extra turning is not needed when an AGA is used. The VM trajectories are almost always superior in terms of TOF because the VVM tends to have more revolutions about the sun, further indicating that the V_∞ turning from Venus and Mars together is sufficient to reach any planet in the solar system.

Mars Free-Return Missions

Recently there has been much interest in exploring Mars. Within the past decade, many missions such as the Mars Global Surveyor, Mars Microprobe, and Mars Polar Lander have been launched.

Table 4   Trajectories to Neptune using AGA at Venus and Mars[a]

Path	Launch date	TOF, yr	Launch V_∞, km/s	Arrival V_∞, km/s	L/D
Low launch V_∞ and short TOF					
VM	27 March 2006	5.4	7.0	28.2	10
VM	10 April 2009	7.1	6.0	23.0	10
M	29 Jan. 2014	7.7	8.0	17.2	10
VM	27 March 2006	6.2	7.0	24.1	7
VM	26 March 2009	7.8	6.0	20.2	7
M	29 Jan. 2014	8.4	8.0	15.5	7
VM	27 March 2006	6.7	8.0	21.8	5
VM	27 March 2006	7.7	7.0	18.2	5
VM	26 March 2009	9.2	6.0	16.1	5
M	29 Jan. 2014	8.6	9.0	15.1	5
Low launch V_∞, short TOF, and low arrival V_∞					
VM	12 March 2006	8.7	6.0	15.5	10
M	29 Jan. 2014	8.8	7.0	14.5	10
VM	24 Feb. 2009	9.3	6.0	16.1	7
VM	16 Sept. 2013	8.9	7.0	15.2	7
M	29 Jan. 2014	9.9	7.0	12.6	7
VM	26 March 2009	9.2	6.0	16.1	5
M	14 Jan. 2014	9.6	8.0	13.1	5
Low launch V_∞ and low arrival V_∞					
VM	18 June 2013	12.8	7.0	9.6	10
M	30 Dec. 2013	12.6	6.0	9.2	10
VM	28 Sept. 2005	12.2	6.0	10.4	7
VMJ	21 May 2007	12.6	6.0	10.2	7
M	14 Jan. 2014	12.8	6.0	9.0	7
VM	1 Oct. 2013	12.9	7.0	9.2	5
M	30 Dec. 2013	12.9	7.0	9.0	5

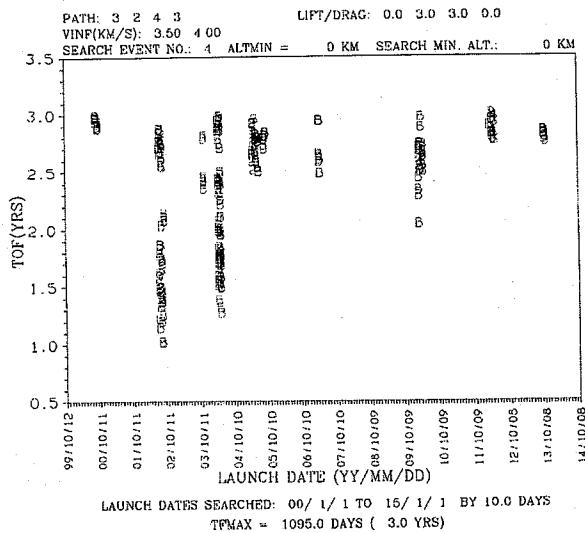[a]Jupiter and Saturn are used for gravity assist alone (i.e., not AGA).

Fig. 8   Mars and Venus free-return trajectories via AGA option at Venus and Mars (or both).
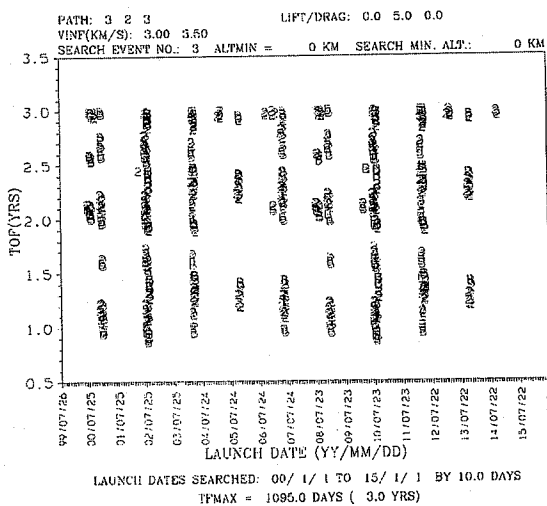

Fig. 9   Venus free-return trajectories via AGA option at Venus.

Aeroassist systems and techniques (such as AGA) will be a vital aspect of these and future missions to Mars.[16]

Figure 8 shows free-return trajectories using Venus and Mars as AGA bodies. Trajectories that use both Venus and Mars make it possible to collect atmospheric samples from both planets in the same mission. The Venus–Mars–Earth (VME) path has low TOF for moderate launch V_∞. The low L/D of 3 makes these trajectories quite promising.

Table 5 gives the best Mars free-return trajectories found by STOUR for a launch period of 1 January 2000 to 1 January 2016. The N/A (not applicable) listing in the L/D column of the first trajectory refers to a pure gravity assist found during the search. Patel[17] and Patel et al.[18] perform extensive research on Mars free-return trajectories for a launch date range of 1 January 1995 to 1 January 2020. They show that trajectories with a 2-year TOF and a launch V_∞ of at least 6.0 km/s exist approximately every two years. References 17 and 18 also present trajectories with very fast TOF (about 1.5 years), but with a high launch V_∞ of 7.0 km/s, and high arrival V_∞ (between 8 and 10 km/s). These trajectories do not occur often, existing only in 2000, 2002, 2015, and 2017 for their 25-year search. If an L/D ratio of 3 is used for the free-return path, shorter TOF exist with even lower launch V_∞. An independent re-creation of the Patel et al.[18] fast trajectories (with STOUR) shows the arrival dates are identical to the arrival dates for the Mars AGA trajecto-

Table 5   Mars free-return trajectories using AGA at Venus and Mars

Path	Launch date	TOF, yr	Launch V_∞, km/s	Arrival V_∞, km/s	L/D
Low launch V_∞ and short TOF					
M	14 June 2003	3.0	3.5	3.5	N/A[a]
M	23 April 2009	3.2	3.0	3.2	1
VM[b]	18 Aug. 2002	1.3	4.0	3.1	1
M	16 March 2001	1.1	3.5	9.5	3
VM	18 Aug. 2002	1.3	4.0	3.3	3
M	16 March 2001	1.0	3.5	9.2	5
VM	18 Aug. 2002	1.2	4.0	4.9	5
M	16 March 2001	1.0	3.5	9.2	7
Low launch V_∞, short TOF, and low arrival V_∞					
M	23 April 2009	3.2	3.0	3.2	1
VM[b]	18 Aug. 2002	1.3	4.0	3.1	1
M	7 Feb. 2010	2.2	4.0	4.5	3
VM	18 Aug. 2002	1.3	4.0	3.3	3
M	28 March 2014	2.4	3.5	4.5	5
M	29 Dec. 2009	2.4	4.0	3.6	5
VM	18 Aug. 2002	1.2	4.0	4.9	5
M	28 March 2014	2.3	3.5	4.2	7
VM[b]	8 Aug. 2002	1.4	4.0	4.5	7
Low launch V_∞ and low arrival V_∞					
M	23 April 2009	3.2	3.0	3.2	1
VM[b]	18 Aug. 2002	1.3	4.0	3.1	1
M	5 April 2001	3.1	3.0	3.5	3
VM	18 Aug. 2002	1.3	4.0	3.3	3
M	26 March 2001	3.1	3.0	3.7	5
M	24 Jan. 2007	3.3	3.0	3.5	7

[a]Pure gravity-assist case is included for comparison.
[b]Only AGA in this trajectory is at Mars.

Table 6   Venus free-return AGA trajectories

Path	Launch date	TOF, yr	Launch V_∞, km/s	Arrival V_∞, km/s	L/D
Low launch V_∞ and short TOF					
V	29 July 2002	1.1	3.0	7.4	N/A[a]
V	29 July 2002	1.0	3.0	6.9	1
V	8 Aug. 2002	1.0	3.0	6.9	3
V	8 Aug. 2002	1.0	3.0	6.8	5
V	8 Aug. 2002	0.9	3.0	6.8	7
Low launch V_∞, short TOF, and low arrival V_∞					
V	15 March 2007	3.3	3.75	2.5	1
V	29 March 2008	3.3	3.5	2.6	3
V	20 April 2000	3.2	3.5	2.7	5
V	21 March 2002	2.4	4.0	3.0	7
V	29 March 2010	3.3	3.25	2.7	7
Low launch V_∞ and low arrival V_∞					
V	15 March 2007	3.3	3.75	2.5	1
V	29 March 2008	3.3	3.5	2.6	3
V	20 April 2000	3.2	3.5	2.7	5
V	29 March 2010	3.3	3.25	2.7	7

[a]Pure gravity-assist case is included for comparison.

ries with TOF of 1.0 year. This comparison supports the notion that the best AGA trajectories listed in Table 5 are simply improved versions (through the use of AGA) of the pure gravity-assist trajectories found by Patel et al. (where AGA reduces launch V_∞ by as much as 4.5 km/s). The arrival V_∞ for the Mars AGA trajectories remains high, but is alleviated in the VM path for the free return. Using the VM path, a TOF of 1.3 years can be obtained with a launch V_∞ of 4.0 km/s and an arrival V_∞ of about 6 km/s less than the best TOF for a pure gravity assist (ME path). In addition to low arrival V_∞, the VM path requires an L/D ratio of only 1 and has a single AGA (occurring at Mars).

Venus Free-Return Missions

Figure 9 plots the Venus free-return trajectories. As expected, the trajectory families repeat about every 1.6 years, the synodic period of Earth and Venus. The best Venus free-return trajectories are listed in Table 6. As with Mars, pure gravity-assist trajectories exist. Interestingly, the AGA trajectories are nearly identical to the

Table 7 Saturn free-return trajectories using AGA at Venus, Mars, and Saturn

Path	Launch date	TOF, yr	Launch V_∞, km/s	Arrival V_∞, km/s	L/D
Low launch V_∞ and short TOF					
VMS	21 May 2007	5.3	5.5	12.5	10
VMS	28 Oct. 2005	7.1	4.5	26.8	10
VMS	21 May 2007	6.4	5.5	19.7	7
VMS	21 May 2007	6.4	6.0	22.2	5
Low Launch V_∞, short TOF, and low arrival V_∞					
VMS	21 May 2007	5.3	5.5	12.5	10
VMS	21 May 2007	6.4	5.5	19.7	7
VMS	21 May 2007	6.4	6.0	22.2	5
Low launch V_∞ and low arrival V_∞					
VMS[a]	19 Aug. 2007	9.1	4.5	11.6	10
VMS[a]	25 March 2012	8.6	5.5	12.3	7
VMS[a]	4 Aug. 2007	9.1	6.0	12.7	5

[a]AGAs in this trajectory are at Mars and Venus (but not Saturn).
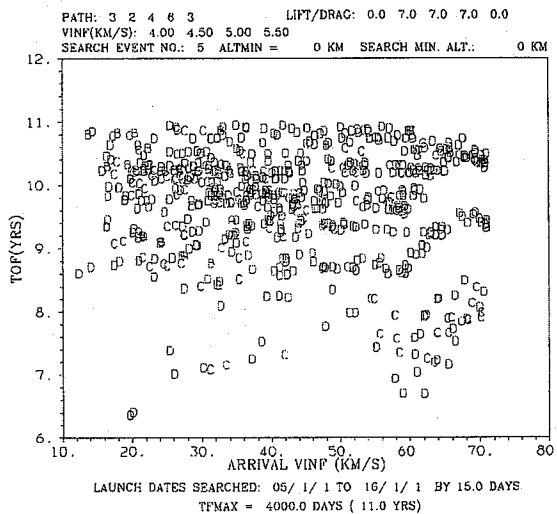
Fig. 10 Saturn free-return trajectories via AGA options at Venus, Mars, and Saturn.

pure gravity assist for the case where the measure of merit is low launch V_∞ and short TOF. Even with increasing L/D ratio, the pure gravity assist is similar to the AGA, indicating that the Venus gravity assist alone provides sufficient V_∞ turning. That the pure gravity assist is comparable to the AGA using the first measure of merit (short TOF and low launch V_∞) does not imply that an AGA cannot improve the trajectory. The trajectories in Table 6, using low arrival V_∞ and low launch V_∞ as the measure of merit, show that very low arrival V_∞ at Earth are achieved using very low L/D.

Saturn Free-Return Missions

Another interesting mission that has yet to receive attention is an atmospheric sample return from Saturn. Atmospheric returns from Saturn could infer the age and chemical evolution of the Saturnian system. The ability of the waverider to capture on return to Earth at high arrival V_∞ is a useful feature of an AGA free-return mission to Saturn. Figure 10 plots Saturn free-return trajectories with L/D ratios of 7. The best free-return trajectories to Saturn are listed in Table 7. We note the exceptional case for an L/D of 10 with a flight time of 5.3 years.

Conclusions

In general, AGA enhances the gravity-assist technique tremendously by reducing launch energy and decreasing flight time. This enhancement depends on the availability of high-L/D hypersonic vehicles, as exemplified by current literature on the waverider. As hypersonic technology improves, providing higher L/D ratios, the launch C_3 and TOF decrease. For example, an L/D ratio of 10

provides a trajectory to Neptune with a C_3 under 50 km²/s² and a TOF of 5.4 years. Conversely, we can study the tradeoff between launch energy and flight time to deep space targets. For example, for an L/D ratio of 7 we can arrive at Pluto in 5 years for a C_3 of 144 km²/s² or we can arrive in 8 years for a C_3 of 56 km²/s². Additionally, our results verify that fast and fuel efficient trajectories to the outer planets can be obtained without using a Jupiter gravity assist. Clearly AGA is an enabling technology that can significantly reduce mission costs, increase science return, and allow greater access to the solar system.

References

[1]Longuski, J. M., "Can Aerogravity-Assist Through the Venusian Atmosphere Permit a Near Radial Trajectory into the Sun?," Jet Propulsion Lab., Rept. EM 312/82-133, California Inst. of Technology, Pasadena, CA, Dec. 1982.

[2]McRonald, A. D., and Randolph, J. E., "Hypersonic Maneuvering for Planetary Gravity Assist," Journal of Spacecraft and Rockets, Vol. 29, No. 2, 1992, pp. 216–222.

[3]Nonweiler, T. R. F., "Aerodynamic Problems of Manned Space Vehicles," Journal of the Royal Aeronautics Society, Vol. 63, Sept. 1959, pp. 521–528.

[4]Gillum, M. J., and Lewis, M. J., "Experimental Results on a Mach 14 Waverider with Blunt Leading Edges," Journal of Aircraft, Vol. 34, No. 3, 1997, pp. 296–303.

[5]Lewis, M. J., and McRonald, A. D., "Design of Hypersonic Waveriders for Aeroassisted Interplanetary Trajectories," Journal of Spacecraft and Rockets, Vol. 29, No. 5, 1992, pp. 653–660.

[6]Bender, D. F., "Trajectories to the Outer Planets Using Aero-Gravity Assist Flybys of Venus and Mars," American Astronautical Society, AAS Paper 91-419, Aug. 1991.

[7]Randolph, J. E., and McRonald, A. D., "Solar System 'Fast Mission' Trajectories Using Aerogravity Assist," Journal of Spacecraft and Rockets, Vol. 29, No. 2, 1992, pp. 223–232.

[8]Sims, J. A., "Delta-V Gravity-Assist Trajectory Design: Theory and Practice," Ph.D. Dissertation, School of Aeronautics and Astronautics, Purdue Univ., West Lafayette, IN, Dec. 1996.

[9]Vinh, N. X., Busemann, A., and Culp, R. D., Hypersonic and Planetary Entry Flight Mechanics, 1st ed., Univ. of Michigan Press, Ann Arbor, MI, 1980, Chap. 2, pp. 19–28.

[10]Miele, A., Flight Mechanics-Volume 1. Theory of Flight Paths, Addison Wesley Longman, Reading, MA, 1962, p. 77.

[11]Bonfiglio, E. P., "Automated Design of Gravity-Assist and Aerogravity-Assist Trajectories," M.S. Thesis, School of Aeronautics and Astronautics, Purdue Univ., West Lafayette, IN, Aug. 1999.

[12]Rinderle, E. A., "Galileo User's Guide, Mission Design System, Satellite Tour Analysis and Design Subsystem," Jet Propulsion Lab., Rept. JPL D-263, California Inst. of Technology, Pasadena, CA, July 1986.

[13]Williams, S. N., "Automated Design of Multiple Encounter Gravity-Assist Trajectories," M.S. Thesis, School of Aeronautics and Astronautics, Purdue Univ., West Lafayette, IN, Aug. 1990.

[14]Longuski, J. M., and Williams, S. N., "Automated Design of Gravity-Assist Trajectories to Mars and the Outer Planets," Celestial Mechanics and Dynamical Astronomy, Vol. 52, No. 3, 1991, pp. 207–220.

[15]Sims, J. A., Staugler, A. J., and Longuski, J. M., "Trajectory Options to Pluto via Gravity Assists from Venus, Mars, and Jupiter," Journal of Spacecraft and Rockets, Vol. 34, No. 3, 1997, pp. 347–353.

[16]Braun, R. D., "Aeroassist Systems: An Important Element in NASA's New Era of Planetary Exploration," Journal of Spacecraft and Rockets, Vol. 36, No. 3, 1999, p. 297.

[17]Patel, M. R., "Automated Design of Delta-V Gravity-Assist Trajectories for Solar System Exploration," M.S. Thesis, School of Aeronautics and Astronautics, Purdue Univ., West Lafayette, IN, Aug. 1990.

[18]Patel, M. R., Longuski, J. M., and Sims, J. A., "Mars Free Return Trajectories," Journal of Spacecraft and Rockets, Vol. 35, No. 3, 1998, pp. 350–354.